Available online at www.sciencedirect.com
ScienceDirect
Trans. Nonferrous Met. Soc. China 23(2013) 1304−1313
Transactions of Nonferrous Metals Society of China
www.tnmsc.cn

Thermal properties of pressureless melt infiltrated AlN−Si−Al composites

Ayse KALEMTAS[1], Gulsum TOPATES[2], Ozlem BAHADIR[2], Pinar KAYA ISCI[2], Hasan MANDAL[3]

1. Department of Metallurgical and Materials Engineering, Mugla Sitki Kocman University, Mugla, Turkey;
2. Department of Materials Science and Engineering, Anadolu University, Eskisehir, Turkey;
3. Material Science and Engineering Programme, Sabanci University, Istanbul, Turkey

Received 27 July 2012; accepted 10 January 2013

Abstract: Thermal properties of AlN−Si−Al composites produced by pressureless melt infiltration of Al/Al alloys into porous α-Si_3N_4 preforms were investigated in a temperature range of 50−300 °C. SEM and TEM investigations revealed that the grain size of AlN particles was less than 1 μm. In spite of sub-micron grain size, composites showed relatively high thermal conductivity (TC), 55−107 W/(m·K). The thermal expansion coefficient (CTE) of the composite produced with commercial Al source, which has the highest TC of 107 W/(m·K), was 6.5×10^{-6} K^{-1}. Despite the high CTE of Al (23.6×10^{-6} K^{-1}), composites revealed significantly low CTE through the formation of Si and AlN phases during the infiltration process.

Key words: AlN; ceramic-matrix composites; thermal properties; liquid metal infiltration

1 Introduction

AlN possesses high thermal conductivity (TC) of 150−200 W/(m·K) [1], low thermal expansion coefficient (CTE) of 4.5×10^{-6} $°C^{-1}$ [1], high electrical resistivity of 10^{14} Ω·cm [2], low dielectric constant of 8.7 at 1 MHz [2], high melting temperature and good oxidation resistance at elevated temperatures [3]. Moreover, AlN has the advantage of a relatively low density, good resistance to molten metals [4] and being an ecologically safe material [5]. Inspite of these superior properties, high price of fine powder and non-aqueous powder processing procedures exposed to water have restricted widespread usage of AlN ceramics [6]. Also, as same as all other ceramic materials, AlN has a very brittle nature and thus has relatively low fracture toughness. One of the prevailing ways to improve toughness of the ceramic materials is addition of a ductile phase such as Al into brittle ceramic.

Al and its alloys are very attractive candidates as matrices for the production of ceramic reinforced metal composites due to their high TC of 180−230 W/(m·K) [7], low density of 2.7 g/cm^3 [7], capability to be strengthened by precipitation [8], good corrosion resistance [8] and high damping capacity [8]. Also Al alloys are easily processed compared with other high TC metals such as copper [7]. The main drawback of pure Al is its high CTE of 23×10^{-6} K^{-1}, but via alloying with Si, CTE of the alloy can be decreased to some extent (~18×10^{-6} K^{-1}) [7].

AlN−Al composites are preferable for either structural or electronic applications mainly due to their attractive electronic, thermal and mechanical properties [5,9,10]. CTE of AlN−Al composite is similar to silicon and has high TC, thus it can be used in semiconductor packaging in aerospace structures [11]. Owing to their favorable thermal properties, they may also have a potential for refractory applications. Most of the researches on the AlN reinforced Al ceramic−metal composites have been focused on the wetting behavior, processing, mechanical properties and microstructure evolution [3−5,11−26]. AlN/Al composite is a promising candidate for electronic packaging and heat sink applications, thus recent researches on the thermal properties of these materials have increased significantly [4,17,18,21,27−33].

AlN−Al composites can be produced via various solid or liquid state based fabrication methods such as spark plasma sintering [27], pressureless [13], pressure [12] or vacuum [14] infiltration, squeeze casting [34], mechanical alloying [35], gas bubbling method [15], DC arc-discharge method [36] and directed melt nitridation [16]. Pressureless metal infiltration technique is the

Corresponding author: Ayse KALEMTAS; Tel: +90-252-2111917, Fax: +90-252-2111912; E−mail: akalemtas@mu.edu.tr
DOI: 10.1016/S1003-6326(13)62598-4

most attractive processing technique since it can potentially combine low-cost, production of high volume fraction AlN−Al composites with near-net shape. Additionally, this technique also provides uniform distribution of the ceramic phase and high dimensional stability.

AGHAJANIAN et al [13] produced AlN matrix composites by using a pressureless melt infiltration technique. They carried out pressureless infiltration studies with 100% Si_3N_4 and 70% Si_3N_4+30% SiC preforms. It was determined that during the pressureless infiltration process, Al reacted with the Si_3N_4 phase and as a result of this interaction (Eq. (1)), AlN and Si phases were formed as the reaction products. This production technique ensures an economical process for the fabrication of AlN based ceramic−metal composites at relatively low temperatures [13]:

$$Si_3N_4+4Al \rightarrow 4AlN+3Si,$$
$$\Delta G_{1200^\circ C}=-355 \text{ kJ/mol}, \Delta H_{1200^\circ C}=-494 \text{ kJ/mol} \quad (1)$$

In this study, instead of using expensive sub-micron AlN powders, an economical α-Si_3N_4 powder was selected as the ceramic starting material. Sub-micron AlN based ceramic−metal composites were produced by the pressureless melt infiltration of Al and Al alloys into the porous α-Si_3N_4 preforms under an argon gas atmosphere. The aim of this study is to demonstrate the possibility of producing sub-micron AlN (~0.3 μm) based ceramic−metal composites, possessing a relatively high TC and low CTE, which can be considered as a suitable thermal management material, by using an economical α-Si_3N_4 starting powder and pressureless melt infiltration technique.

2 Experimental

Ceramic−metal composites were produced by melt infiltrating the Al/Al alloy blocks (Table 1) into porous α-Si_3N_4 (Silzot HQ, Fig. 1) preforms prepared by uniaxially pressing under 70 MPa. The relative green density values of the ceramic preforms were ~46%. Infiltration process was carried out under an Ar gas atmosphere at 1200 °C for 1 h without applying any external pressure. Heating rates applied was 5 °C/min up to 900 °C and 10 °C/min onwards up to 1200 °C. Cooling rates from 1200 °C to 900 °C was 10 °C/min and then 5 °C/min down to room temperature.

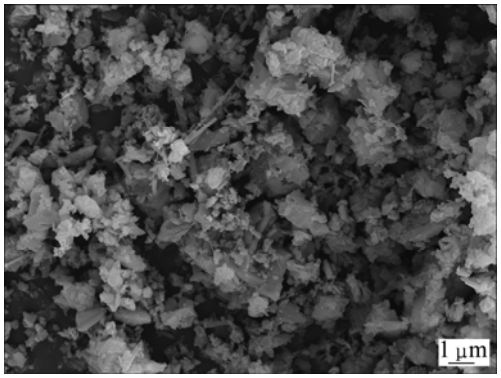

Fig. 1 SEM micrograph of starting α-Si_3N_4 powder

Density of the produced composites was calculated by Archimedes' displacement method. X-ray diffraction (XRD) was performed to identify phases on Rigaku Rint 2200 X-ray instrument by using monochromatic Cu K_α radiation (λ=1.5406 Å). Scanning electron microscopy (SEM) investigations were carried out using Zeiss Supra 50 VP microscope. Samples were prepared through a standard procedure, using mechanical polishing steps, followed by Ar-ion thinning method for transmission electron microscopy (TEM) investigations. Afterwards, the sample was characterized with a 200 kV field emission Jeol 2100F TEM.

The heat capacities of the Al sources and produced composites were calculated via rule of mixtures (ROM) by using the heat capacity at 50−300 °C obtained from the MTDATA thermodynamic program for each component. Thermal diffusivities of the Al sources and produced composites were characterized by laser flash technique (Netzsch−LFA 457) using 10 mm×10 mm×2 mm square samples. Then TC values of these materials were calculated with the equation given below:

$$\lambda=c_p\rho\alpha \quad (2)$$

where λ is the heat capacity; c_p is the specific heat; ρ is density; α is the thermal diffusivity. The coefficient of thermal expansion (CTE) measurements of the samples were performed on a Netzsch−DIL 402 PC dilatometer. The dimensions of the CTE samples were 5 mm×5 mm×40 mm. CTE and thermal diffusion (TD) measurements were done between 25−275 °C and 25−300 °C, respectively. These temperatures are close to typical application temperature for electronic packaging materials.

Table 1 Room temperature properties of used Al sources

Al source	Composition/%	Density/(g·cm^{-3})	Heat capacity*/ (J·g^{-1}·K^{-1})	TC/(W·m^{-1}·K^{-1})
Commercial Al	> 99 Al	2.69	0.90	223
Al−Mg	4.56 Mg	1.73	0.91	129
2024	4.90 Cu−1.80 Mn	2.79	0.89	160
7075	2.30Mg−1.30Cu−5.30 Zn	2.82	0.89	179

*: Theoretically calculated by rule of mixtures as described above.

3 Results

Bulk density and residual open porosity content of composites are given in Table 2. Open porosities of all the samples were below 1% and bulk density of the composites increased slightly (2.84−2.93 g/cm^3) depending on the chemical composition of the used Al source.

Table 2 Bulk density and open porosity of the composites produced with different Al sources.

Al source	Bulk density/ (g·cm^{-3})	Open porosity/%
Commercial Al	2.85±0.01	0.71±0.07
7075	2.86±0.01	0.65±0.05
Al−Mg	2.89±0.01	0.71±0.21
2024	2.92±0.01	0.66±0.09

X-ray diffraction analysis (Fig. 2) of the composites revealed that all samples mainly contain AlN, Al and Si phases. When 2024 alloy was used, it was observed that $CuAl_2$ precipitate phase was also formed (Fig. 2).

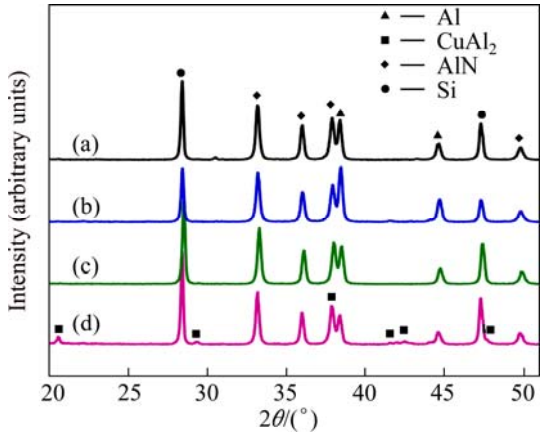

Fig. 2 XRD patterns of ceramic−metal composites produced by using commercial Al metal (a), Al−Mg (b), 7075 Al alloy (c) and 2024 Al alloy (d)

Formation of AlN grains takes place by dissolution of α-Si_3N_4 grains within Al/Al alloy followed by nucleation and growth of AlN grains during the infiltration process. Direct contact between Al and α-Si_3N_4 particles is achieved just after removing the SiO_2 surface layer on the α-Si_3N_4 particles. Surface SiO_2 layer is consumed via reacting with Al phase during the infiltration process.

It was determined that all α-Si_3N_4 phase was consumed during the reactive melt infiltration process (Fig. 2) according to Eq. (1). After the infiltration process, it was observed that needle like Si crystals have grown on the residual Al metal source remaining on surface of the composite. Some of these crystals were several millimeters in size. The released Si metal phase was diffused to the liquid Al source through the interconnected liquid channels and during the cooling process, Si was crystallized in the residual Al metal source.

SEM investigations of the composites indicated that these materials are highly dense and have a very fine (<1 μm) microstructure (Fig. 3). Fracture surface investigations of these composites also revealed that the brittle fracture mode of fine AlN particles and ductile failure mode of Al/Al alloys (Fig. 3). TEM investigations of these samples revealed that the particle size of the AlN is ~300 nm (Fig. 4). These observations (Fig. 5) confirm the XRD results (Fig. 2) which shows that α-Si_3N_4 starting powder is consumed completely during the reactive melt infiltration process. Microstructure investigations demonstrate that in situ formed AlN ceramic particles are distributed uniformly within the Al/Al alloy and therefore it is expected that composites should exhibit isotropic properties.

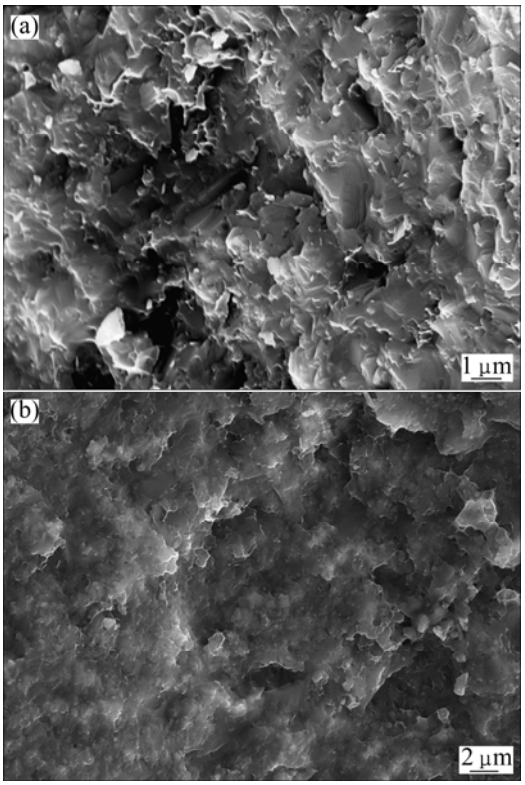

Fig. 3 SEM images of fracture surface of produced composites by using commercial Al (a) and 2024 Al alloy (b)

The contents of the AlN, Si and Al of the composites were calculated according to Eq. (1) considering the green density of the porous α-Si_3N_4

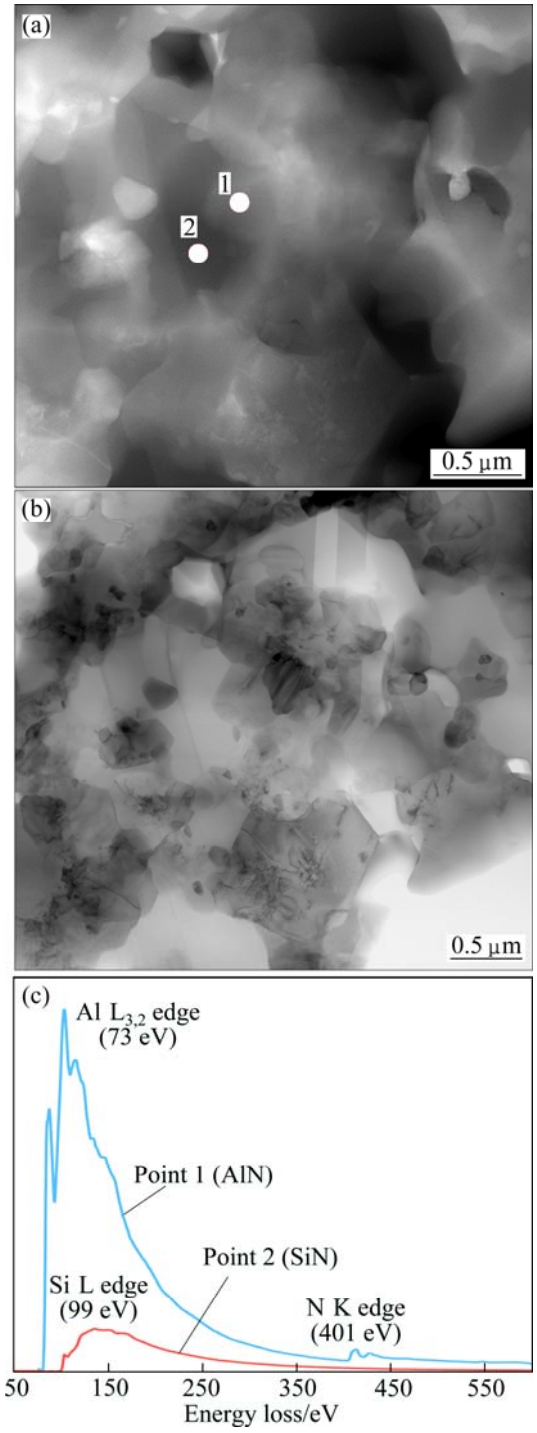

Fig. 4 STEM HAADF (a) and BF (b) images showing microstructure of composite produced by using commercial Al, and EELS spectra (c) of Al $L_{3,2}$ edge, Si L edge and N K edge collected from grains labeled as "1" and "2" in (a)

ceramic preforms. Phase content of the composites was calculated by the following assumptions.

1) Voids of the porous α-Si_3N_4 pellets were fully filled with Al/Al alloys during the infiltration step.

2) α-Si_3N_4 starting powder is consumed completely (Figs. 2 and 5) during the reactive melt infiltration process according to Eq. (1).

3) Phase assemblage of the composites includes only AlN, Al and Si (Fig. 2).

4) Diffusion of the released Si to the Al source is ignored.

Composition of the composite produced using commercial Al metal is calculated at aforementioned conditions as 11.1%Al, 37.2%Si and 51.7%AlN (in volume fraction).

TD values of composites in the temperature range of 25−300 °C are given in Fig. 6. All TD values of the samples decrease with increasing the temperature. Composite produced with a commercial Al source has the highest TD value of ~42×10^{-6} m^2/s at the room temperature; while the lowest value is ~21×10^{-6} m^2/s obtained for the composite produced with an Al−Mg alloy.

Figure 7 shows variation of TC values of the composites depending on the temperature. TC values of composites were directly affected by the composition and TC of the Al source. With commercial Al that contained the lowest impurity amount, the prepared composite had the highest TC value of 107 W/(m·K). Moreover, with increasing the TC value of Al source, TC values of the composites were enhanced. The lowest TC value was obtained as 55 W/(m·K) for Al−Mg alloy that has the lowest TC value among the Al sources used.

TC of the ceramic−metal composites is provided by the electron and phonon conduction. Electron thermal conduction is the dominant conduction mechanism for the metal components such as Al. Phonon conduction, the dominant conduction mechanism for the electrically insulating AlN ceramic, can be ignored for the metal phases.

Each individual component of composite has very high TC (Table 3). However, actually measured TC values of composites (Fig. 7) are remarkably lower compared with AlN, Al and/or Si (Table 3). This behavior can be explained mainly by the following effects.

3.1 General properties of composite

TC of the produced ceramic−metal composites is significantly affected by the connectivity of the phases and porosity of the material.

3.1.1 Connectivity of phases

The difficulty of achieving homogenous distribution of the major phases (AlN, Al and Si) reduced the connectivity of the phases which lower the TC. The other reason for the poor TC was the reduction in the amount of Al phase as a result of the substantial consumption of Al during the infiltration process. Besides them, sub-micron particle size of in-situ formed AlN also reduced the TC values of composites.

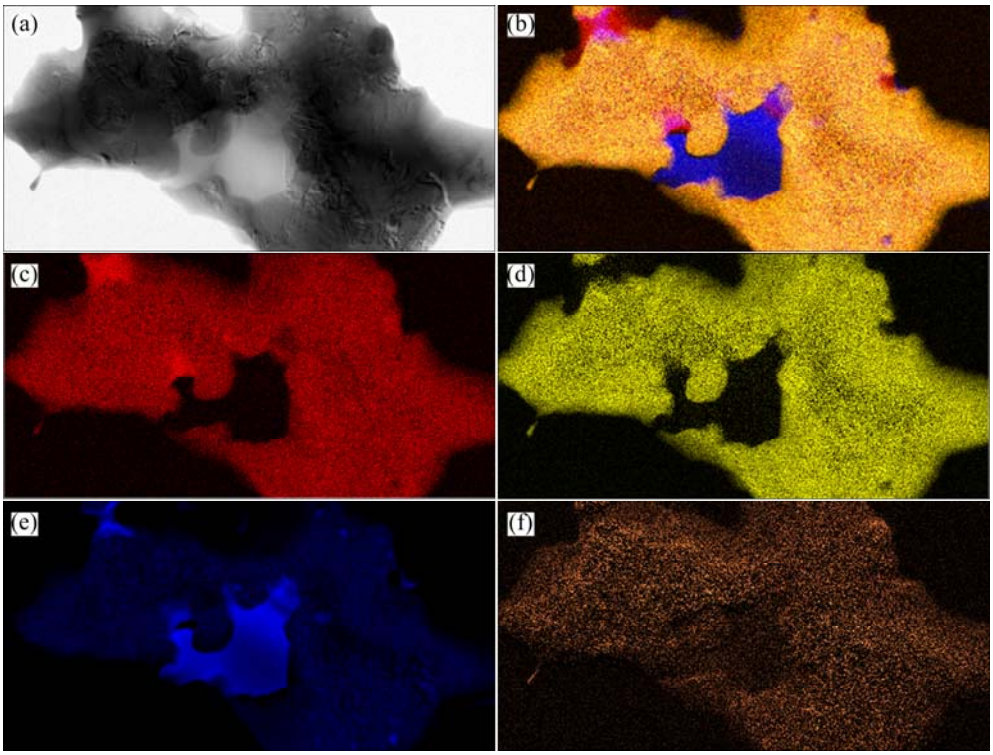

Fig. 5 EFTEM 3 window elemental mapping showing zero loss image (± 20 eV) (a), general distribution of Al, N, Si and O elements (b), Al K edge (1560 eV) (c), N K edge (401 eV) (d), Si L edge (99 eV) (e) and O K edge (532 eV) (f)

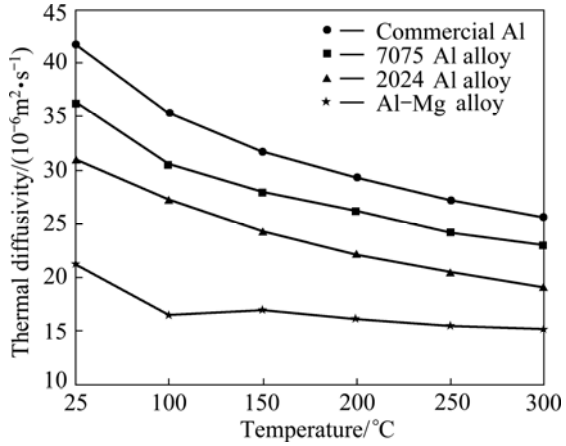

Fig. 6 TD of the composites as function of temperature

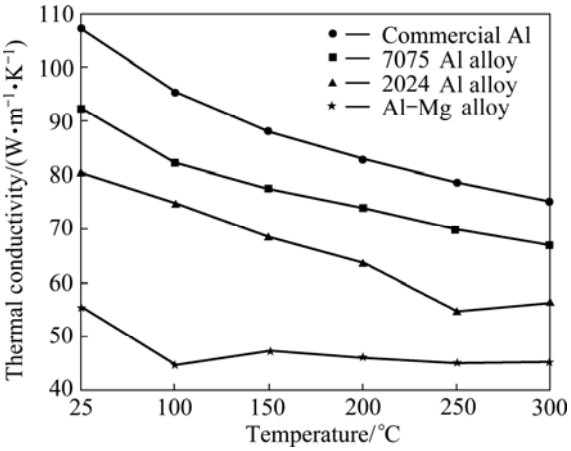

Fig. 7 TC variation of the composites with temperature

Table 3 Some selected properties of AlN, Si and Al materials

Material	Density/ ($g \cdot cm^{-3}$)	CTE/ ($10^{-6}°C^{-1}$)	TC/ ($W \cdot m^{-1} \cdot K^{-1}$)	*K*/ GPa	*G*/ GPa
AlN	3.26 [37]	4.3 [39]	120−210 [39]	200 [37]	130 [37]
Si	2.33 [38]	2.5 [38]	141 [38]	100 [41]	52 [43]
Al	2.71 [38]	23.6 [38]	237 [40]	67.6 [42]	25.9 [42]

K: Bulk modulus; *G*: Shear modulus.

3.1.2 Porosity

Porosity of the composite material can considerably decrease the TC via enhancing the phonon scattering [27,44]. DUN et al [27] reported that even a relatively low improvement (1.9%, from 97.1% to 99.0%) in the density of the AlN/Al composite produced via spark plasma sintering resulted in a significant improvement (25.1 W/(m·K)) in the TC of the composite and 97.5 W/(m·K) was obtained for the 99% dense material. TC of the AlN/Al composite is very sensitive to the relative density of the material [27] and composite produced in this work is ~99%. Thus, further improvement of the densification probably may improve the TC of the produced composite.

3.2 Properties of ceramic phase

Initial ceramic powder properties (α-Si_3N_4), as well as the end-product ceramic phase (AlN), have an essential effect on the TC of the composite material. Especially, particle size and impurity level of the starting

α-Si_3N_4 powder have a remarkable effect on the TC.

3.2.1 Particle size of ceramic phase

When the particle size decreased to sub-micron size, a substantial increase in the grain boundary volume occurs. Increasing grain boundary volume resulted in the enhanced scattering of the conducting electrons, leading to a lower TC. The grain boundaries reduce the TC by decreasing either the mean free path (MFP) or the effective electron density along the MFP [45]. Smaller grain size induces more interfacial thermal resistance compared to coarse grain size counterparts since interface volume fraction is inversely proportional to the grain size. Therefore, TC decreases with reducing the grain size of the ceramic particles in the composite. SEM (Fig. 3) and further TEM (Fig. 4) studies revealed that composites produced in this study contain very fine AlN grains (~300 nm). In spite of sub-micron AlN grain size, the TC values attained for the produced ceramic−metal composites (Fig. 7) are sufficient for electronic packaging application [4].

3.2.2 Intrinsic properties of ceramic phase

Theoretical TC of pure single crystal AlN is calculated to be 320 W/(m·K) at room temperature [46]. However, actually determined TC of polycrystalline AlN ceramics has a notably lower value. Material characteristics such as temperature, impurities, grain size, porosity and preferred orientation affect the phonon MFP, thereby changing TC [47,48]. When the frequency of phonon scattering increases, TC reduces because the phonon MFP is decreased. TC (k) of AlN can be expressed by

$$k=\frac{1}{3}C\nu\langle l\rangle \tag{3}$$

where C is the heat capacity of AlN; ν is the phonon velocity; $\langle l\rangle$ is the phonon MFP [49−51].

During the formation of AlN particles, some impurities may be incorporated into the lattice and also some defects within the phase lattice may be formed, which may have a detrimental effect on the TC of the in-situ formed AlN grains. Particularly, the lattice-dissolved oxygen has a substantial decrease on the TC of AlN and TC of AlN is inversely proportional to the oxygen content dissolved in the AlN lattice [49,27]. When oxygen diffuses into the lattice at high temperatures, Al vacancies are formed, then the TC of the polycrystalline AlN ceramics decreases by enhancing the phonon scattering. Impurities such as oxygen are solid-dissolved in AlN crystal lattices or a composite oxide forms, such as Al−O−N, which hinders the propagation of the thermal oscillations of the lattice. These impurities are incorporated into the AlN lattice by substitutional solution in the nitrogen site, creating aluminum vacancies, according to the following reaction (Eq. (4)) [52]:

$$Al_2O_3\longrightarrow 2Al_{Al}+[\cdot]_{Al}+3O_N \tag{4}$$

where $[\cdot]_{Al}$ denotes an Al vacancy. Vacant Al site can cause mass and strain misfits. These misfits increase the scattering cross section of phonons, which decreases the phonon MFP, thereby lowering the TC [52].

TC of the AlN ceramic is inversely proportional to the formation of Al vacancies and even at low concentrations, oxygen promotes the formation of Al vacancies and thus decreases the TC of the AlN [53]. Al vacancy concentrations is directly proportional to the oxygen concentration and with increasing the oxygen concentration and coalescence of Al vacancies, formation of stacking faults and some other defects also increases, which in turn decreases the TC of the material [54].

YU et al [55] reported that secondary phases along grain boundaries or at grain junctions have a detrimental influence on the TC of AlN materials and microstructural changes are found to disrupt the connection between the AlN grains, resulting in a decrease in the TC of the materials. AlN−Si−Al composite system has different phase contents, thus the presence of distinct phases between the AlN grains may lead to a appreciable decrease in the TC of the material.

3.3 CTE of AlN−Si−Al ceramic−metal composites

Al has a very high CTE compared with AlN and Si phases, which are formed via the reaction between α-Si_3N_4 and Al during the pressureless melt infiltration process, and have very low CTE (Table 3). Figure 8 depicts the measured CTE values of the composites produced with commercial Al and 2024 Al alloy metal sources at temperatures varying from 25 °C to 275 °C.

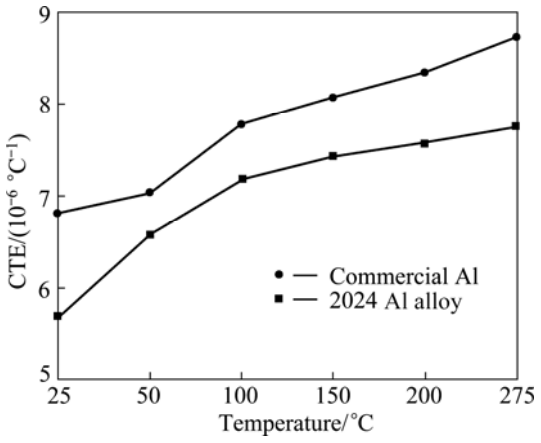

Fig. 8 CTE variation of AlN−Si−Al ceramic−metal composites produced with commercial Al and 2024 Al alloy with temperature.

As is clearly seen from Fig. 8, room temperature CTE of the composite produced with commercial Al source is 6.8×10^{-6} °C^{-1} whereas it is 8.7×10^{-6} °C^{-1} at 275 °C. This value is significantly low compared with the CTE of the commercial Al or Al alloys (Table 3). Composite produced with 2024 Al alloy has even a lower CTE of 5.7×10^{-6} °C^{-1} at room temperature and 7.8×10^{-6} °C^{-1} at 275 °C. This effect is attributed to the formation of Si and AlN phases during the infiltration process which has low CTE values (Table 3) and prevents the expending of Al phase during the thermal expansion process. The CTE of the produced composites (Fig. 8) is very close to that of Al_2O_3 (8×10^{-6} °C^{-1}) [4], which is a commonly used material for electronic substrates.

3.3.1 CTE models

The measured CTE of the composites were compared with the theoretical predictions calculated according to the ROM and Turner [56] models (Table 4). The first scientist who took the elastic constant into account to calculate the CTE is TURNER (Eq. (6)) and the predicted CTE value by this model is lower than that by ROM prediction. According to ROM, the simplest theoretical CTE prediction model, the CTE of the composite, produced by using a commercial Al source, is calculated as 5.8×10^{-6} °C^{-1} at room temperature. The calculated CTE value for the same composite by the Turner model is lower than that by ROM approximation, 4.8×10^{-6} °C^{-1}. Both these values are lower than the measured CTE of the composite, 6.8×10^{-6} °C^{-1} [57].

Table 4 Theoretical prediction models used in this study to determine CTE

Model	Predictions	
ROM	$\alpha_c=\alpha_{p1}V_{p1}+\alpha_{p2}V_{p2}+\alpha_m V_m$	(Eq. 5)
TURNER [56]	$\alpha_c=\dfrac{\alpha_m K_m V_m+\alpha_{p1}K_{p1}V_{p1}+\alpha_{p2}K_{p2}V_{p2}}{K_m V_m+K_{p1}V_{p1}+K_{p2}V_{p2}}$	(Eq. 6)

K: Bulk modulus; V: Volume fraction; Subscript c: Composite; Subscript m: Matrix phase; Subscript p: Second phase.

3.3.2 Comparison of achieved CTE and TC values with literature data

In this study, AlN−Si−Al ceramic−metal composites are produced by pressureless reactive melt infiltration process and an economical α-Si_3N_4 starting powder was used instead of expensive sub-micron AlN powders.

A short summary of the literature survey about the CTE and TC of AlN/Al composites is given in Table 5. ZHANG et al [32] used coarser AlN starting powder and achieved a higher TC value but also a higher CTE value (Table 5). In this study, a simple production technique was used. However, achieved CTE and TC values are readily comparable with the counterparts produced via

Table 5 CTE and TC of various AlN/Al composites produced via different production techniques with AlN or Si_3N_4 starting powders

Starting powder	Volume fraction/%	Particle	Production method and conditions	CTE/ 10^{-6} °C	TC/(w·m^{-1}·K^{-1})	Reference
AlN	85	AlN: 1−10 μm Al: 10−60 μm	Spark plasma sintering (at 1550 °C for 5 min under 70 MPa)		97.5	[27]
	20	AlN: 0.4 μm Al: 71 μm	Hot extrusion			[28]
	4, 8, 15, 24, 30, 39	AlN/Al nanoparticles	Production of AlN/Al nanoparticles by arc-discharge plasma evaporation followed by hot pressing (500 °C, 1 GPa, in vacuum of 10^{-4} Pa)	13.9	50 (39%)	[29]
	50	AlN: 4 μm	Squeeze casting	11.2	130	[32]
	42, 45, 48		Squeeze casting at 130 MPa	6.5 (AlMgSi0.5−42% HCS AlN) 8.6 (AlMg3−48% HCS AlN) 8.9 (AlCu4Mg1−45% ESK AlN)	131 (AlMgSi0.5−42% HCS AlN) 85 (AlMg3−48% HCS AlN) 89 (AlCu4Mg1−45% ESK AlN)	[33]
	56.5	AlN: 1.5 μm		9	100	[4]
Si_3N_4	36	Si_3N_4: 0.2 μm	Pressure infiltration method		95	[30]
	61.9		Pressure infiltration at 800 °C and 90 MPa with presintered Si_3N_4 pellets used	7.3	75	[21]

expensive production techniques and by using high purity starting materials (Table 5).

4 Conclusions

1) The main attractive features of the produced AlN−Si−Al ceramic−metal composites are high densification rate (~99%), low density (2.84−2.93 g/cm^3), utilizing the near net shape capability of pressureless reactive melt infiltration process and usage of an economical α-Si_3N_4 starting powder instead of expensive sub-micron AlN powders.

2) Composite produced with a commercial Al source has the highest TC value, 107 W/(m·K), which is enough for the heat dissipation of the electronic substrates [4], even though produced composite consists of sub-micron in-situ formed AlN grains.

3) Generally, recommended CTE values for the thermal management materials used in electronics packaging are between 4×10^{-6} and 7×10^{-6} °C^{-1} to match the CTE of semiconductors. CTE value for pure Al is very high but produced composites possess fairly low CTE values, $(5.8-6.8)\times10^{-6}$ °C^{-1}, which is suitable to be used as the thermal management materials.

4) Overall properties attained for the produced composites are sufficient for electronic packaging application.

Acknowledgements

We are grateful to The Foundation for Scientific Research Projects of Mugla Sitki Kocman University (Project No. 10/30) and The Scientific & Technological Research Council of Turkey (TUBITAK, Project No: 108M194) for funding the present work. We also would like to acknowledge MSc student Serkan Ulukut (Anadolu University) for his help during the TEM sample preparation studies.

References

[1] MROZ T J. Annual minerals review: Aluminum nitride [J]. The Bulletin of the American Ceramic Society, 1994, 73(6): 77.

[2] XIE S H, ZHU B K, LI J B, WEI X, XU Z K. Preparation and properties of polyimide/aluminum nitride composites [J]. Polymer Testing, 2004, 23(7): 797−801.

[3] SALAHI E, HEINRICH J G. Correlation between nitriding process and microstructure of reaction bonded aluminum nitride ceramics [J]. British Ceramic Transactions, 2003, 102: 161−168.

[4] COUTURIER R, DUCRET D, MERLE P, DISSON J P, JOUBERT P. Elaboration and characterization of a metal matrix composite: Al/AlN [J]. Journal of the European Ceramic Society, 1997, 17(15−16): 1861−1866.

[5] ZHANG G A, WU Z G, WANG M X, FAN X Y, WANG J, YAN P X. Structure evolution and mechanical properties enhancement of Al/AlN multilayer [J]. Applied Surface Science, 2007, 253: 8835−8840.

[6] PATHAK L G, RAY A K, DAS S, SIVARAMAKRISHNAN C S, RAMACHANDRARAO P. Carbothermal synthesis of nanocrystalline aluminum nitride powders [J]. Journal of the American Ceramic Society, 1999, 82(1): 257−260.

[7] ELLIS D L, MCDANIELS D L. Thermal conductivity and thermal expansion of graphite fiber−reinforced copper matrix composites [J]. Metallurgical and Materials Transactions A, 1993, 24: 43−52.

[8] CAYRON C. TEM study of interfacial reactions and precipitation mechanisms in Al_2O_3 short fiber or high volume fraction SiC particle reinforced Al−4Cu−1Mg−0.5Ag squeeze-cast composites [D]. Lausanne: École Polytechnique Fédérale de Lausanne, 2000.

[9] CHENG H, HING P. The evolution of preferred orientation and morphology of AlN films under various RF sputtering powers [J]. Surface and Coatings Technology, 2003, 167(2−3): 297−301.

[10] OLIVEIRA I C, GRIGOROV K G, MACIEL H S, MASSI M, OTANI C. High textured AlN thin films grown by RF magnetron sputtering: Composition, structure, morphology and hardness [J]. Vacuum, 2004, 75(4): 331−338.

[11] ABDOLI H, SALAHI E, FARNOUSH H, POURAZRANG K. Evolutions during synthesis of Al−AlN-nanostructured composite powder by mechanical alloying [J]. Journal of Alloys and Compounds, 2008, 461(1−2): 166−172.

[12] CHEDRU M, VICENS J, CHERMANT J L, MORDIKE B L. Aluminium–aluminium nitride composites fabricated by melt infiltration under pressure [J]. Journal of Microscopy, 1999, 196(2): 103−112.

[13] AGHAJANIAN M K, BIEL J P, SMITH R G. AlN matrix composites fabricated via an infiltration and reaction approach [J]. Journal of the American Ceramic Society, 1994, 77(7): 1917−1920.

[14] LAI S W, CHUNG D D. Super high-temperature resistance of aluminum nitride particle-reinforced aluminum compared to silicon carbide or aluminum particle-reinforced aluminum [J]. Journal of Materials Science, 1994, 24: 6181−6198.

[15] ZHENG Q, REDDY R G. Kinetics of in-situ formation of AlN in Al alloy melts by bubbling ammonia gas [J]. Metallurgical and Materials Transactions B, 2003, 34: 793−804.

[16] KONDOH K, TAKEDA Y, KIMURA A. Wear properties of in-situ reacted Al−AlN composite sintered material and application for automatic transmission parts [J]. SAE Transactions: Journal of Materials and Manufacturing, 1999, 108: 917−921.

[17] LIU Y Q, CONG H T, WANG W, SUN C H, CHENG H M. AlN nanoparticle-reinforced nanocrystalline Al matrix composites: Fabrication and mechanical properties [J]. Materials Science and Engineering A, 2009, 505(1−2): 151−156.

[18] BODDAPATI SR, RÖDEL J, JAYARAM V. Crack growth resistance (R-curve) behaviour and thermo-physical properties of Al_2O_3 particle-reinforced AlN/Al matrix composites [J]. Composites Part A: Applied Science and Manufacturing, 2007, 38(3): 1038−1050.

[19] CHEÂDRU M, VICENS J, CHERMANT J L, MORDIKE B L. Transmission electron microscopy studies of squeeze cast Al−AlN composites [J]. Journal of Microscopy, 2001, 201: 299−315.

[20] ZHAO M, WU G, ZHU D, JIANG L, DOU Z. Effects of thermal cycling on mechanical properties of AlNp/Al composite [J]. Materials Letters, 2004, 58: 1899−1902.

[21] KAWAI C, PARK J J. Mechanical and thermal properties of Al−Si_3N_4 composites fabricated by the infiltration of molten Al into a porous Si_3N_4 ceramic with network [J]. Journal of Materials Science Letters, 2001, 20(4): 385−388.

[22] KEVORKIJAN V M. The reactive infiltration of porous ceramic media by a molten alumium alloy [J]. Composites Science and Technology, 1999, 59(5): 683−686.

[23] KEVORKIJAN V M, TORKAR M, SUSTARSIC B. Modeling of the reactive immersion of ceramic particles into molten aluminium alloys [J]. Composites Science and Technology, 1999, 59(10): 1503−1511.

[24] ZHAO J Z, GAO J Q, JIN Z H. Preparation of AlN matrix composites using an infiltration and reaction approach [J]. Materials Chemistry and Physics, 2006, 97(2−3): 506−510.

[25] de la PENA J L, PECH-CANUL M I. A reactive wetting and spreading of Al−Si−Mg alloys on Si_3N_4/Si substrates [J]. Materials Science and Engineering A, 2008, 491: 461−469.

[26] de la PENA J L, PECH-CANUL M I. Wetting behavior of Al−Si−Mg alloys on Si_3N_4/Si substrates: Optimization [J]. Applied Physics A: Materials Science & Processing, 2008, 91(3): 545−550.

[27] DUN B, JIA X, JIA C, CHU K. Thermal conductivity behavior of SPS consolidated AlN/Al composites for thermal management applications [J]. Rare Metals, 2011, 30(2): 189−194.

[28] WANG J, YI D, SU X, YIN F, LI H. Properties of submicron AlN particulate reinforced aluminum matrix composite [J]. Materials and Design, 2009, 30(1): 78−81.

[29] LIU Y Q, CONG H T, CHENG H M. Thermal properties of nanocrystalline Al composites reinforced by AlN nanoparticles [J]. Journal of Materials Research, 2009, 24(1): 24−31.

[30] YANG Wen-shu, XIU Zi-gang, CHEN Guo-qin, WU Gao-hui. Microstructure and thermal conductivity of submicron Si_3N_4 reinforced 2024Al composite [J]. Transactions of Nonferrous Metals Society of China, 2009, 19(s2): s378−s381.

[31] RAO V V, KRISHNA MURTHY M V, NAGARAJU J. Thermal conductivity and thermal contact conductance studies on Al_2O_3/Al−AlN metal matrix composite [J]. Composites Science and Technology, 2004, 64(16): 2459−2462.

[32] ZHANG Q, CHEN G, WU G, XIU Z, LUAN B. Property characteristics of a AlN_p/Al composite fabricated by squeeze casting technology [J]. Materials Letters, 2003 57(8): 1453−1458.

[33] CHÉDRU M, CHERMANT J L, VICENS J. Thermal properties and Young's modulus of Al−AlN composites [J]. Journal of Materials Science Letters, 2001, 20(10): 893−895.

[34] LII D F, HUANG J L, CHANG S T. The mechanical properties of AlN/Al composites manufactured by squeeze casting [J]. Journal of the European Ceramic Society, 2002, 22(2): 253−261.

[35] TROADEC C, GOEURIOT P, VERDIER P, LAURENT Y, VICENS J, BOITIER G, CHERMANT J L, MORDIKE B L. AlN dispersed reinforced aluminum composite [J]. Journal of the European Ceramic Society, 1997, 17(15−16): 1867−1875.

[36] YU San, LI Dong-mei, SUN Hai-ping, LI Hong-dong, YANG Hai-bin, ZOU Guang-tian. Microanalysis of single-phase A1N nanocrystals and AlN−Al nanocomposites prepared by DC arc-discharge [J]. Journal of Crystal Growth, 1998, 183(3): 284−288.

[37] DODD S P, SAUNDERS G A, CANKURTARAN M, JAMES B. Ultrasonic study of the elastic and nonlinear acoustic properties of ceramic aluminum nitride [J]. Journal of Materials Science, 2001, 36(3): 723−729.

[38] CALLISTER W D. Materials science and engineering: An introduction [M]. 6th ed. New York: John Wiley & Sons Inc, 2003.

[39] CARTER B C, NORTON M G. Ceramic materials science and engineering [M]. New York: Springer, 2007.

[40] ELOMARI S, SKIBO M D, SUNDARRAJAN A, RICHARDS D. Thermal expansion behavior of particulate metal-matrix composites [J]. Composites Science and Technology, 1998, 58(3−4): 369−376.

[41] LAM P K, COHEN M L, MARTINEZ G. Analytic relation between bulk moduli and lattice constants [J]. Physical Review B, 1987, 35(17): 9190−9194.

[42] TORQUATO S, YEONG C L Y, RINTOUL M D, MILIUS D L, AKSAY I A. Elastic properties and structure of interpenetrating boron carbide/aluminum multiphase composites [J]. Journal of the American Ceramic Society, 1999, 82(5): 1263−1268.

[43] WORTMAN J J, EVANS R A. Young's modulus, shear modulus, and Poisson's ratio in silicon and germanium [J]. Journal of Applied Physics, 1965, 36(1): 153−156.

[44] CHU K, JIA C C, TIAN W H, LIANG X B, CHEN H, GUO H. Thermal properties of carbon nanotube−copper composites for thermal management applications [J]. Nanoscale Research Letters, 2010, 5(5): 868−874.

[45] QIN X Y, WU B M, DU Y L, ZHANG L D, TANG H X. An experimental study on thermal diffusivity of nanocrystalline Ag [J]. Nanostructured Materials, 1996, 7(3): 383−391.

[46] SLACK G A. Nonmetallic crystals with high thermal conductivity [J]. Journal of Physics and Chemistry of Solids, 1973, 34(2): 321−335.

[47] KINGERY W D, BOWEN H K, UHLMANN D R. Introduction to ceramics [M]. 2nd ed. New York: Wiley, 1976.

[48] BOEY F, TOK A I Y, LAM Y C, CHEW S Y. On the effects of secondary phase on thermal conductivity of AlN ceramic substrates using a microstructural modeling approach [J]. Materials Science and Engineering A, 2002, 335(1−2): 281−289.

[49] SLACK G A, TANZILLI R A, POHL R O, VANDERSANDE J W. The intrinsic thermal-conductivity of AlN [J]. Journal of Physics and Chemistry of Solids, 1987, 48(7): 641−647.

[50] RUCKMICH S, KRANZMANN A, BISCHOFF E, BROOK R J. A description of microstructure applied to the thermal conductivity of AlN substrate materials [J]. Journal of the European Ceramic Society, 1991, 7(5): 335−341.

[51] WATARI K, ISHIZAKI K, FUJIKAWA T. Thermal conduction mechanism of aluminium nitride ceramics [J]. Journal of Materials Science, 1992, 27(10): 2627−2630.

[52] OLHERO S M, MIRANZO P, FERREIRA J M F. Influence of the de-waxing atmosphere on the properties of AlN ceramics processed from aqueous media [J]. Journal of the European Ceramic Society, 2006, 26(13): 2475−2483.

[53] SLACK G A, SCHOWALTER L J, MORELLI D, FREITAS J A. Some effects of oxygen impurities on AlN and GaN [J]. Journal of Crystal Growth, 2002, 246(3−4): 287−298.

[54] HARRIS J H, YOUNGMAN R A, TELLER R G. On the nature of the oxygen-related defect in aluminum nitride [J]. Journal of Materials Research, 1990, 5(8): 1763−1773.

[55] YU Y D, HUNDERE A M, HØIER R, BORKOWSKI R D, EINARSRUD M A. Microstructural characterization and microstructural effects on the thermal conductivity of AlN(Y_2O_3) ceramics [J]. Journal of the European Ceramic Society, 2002, 22(2): 247−252.

[56] TURNER P S. Thermal expansion stresses in reinforced plastics [J]. Journal of Research of the National Bureau of Standards, 1946, 37: 239−250.

[57] MALLIK S, EKERE N, BEST C, BHATTI R. Investigation of thermal management materials for automotive electronic control units [J]. Applied Thermal Engineering, 2011, 31(2−3): 355−362.

无压熔渗 AlN−Si−Al 复合材料的热性能

Ayse KALEMTAS[1], Gulsum TOPATES[2], Ozlem BAHADIR[2], Pinar KAYA ISCI[2], Hasan MANDAL[3]

1. Department of Metallurgical and Materials Engineering, Mugla Sitki Kocman University, Mugla, Turkey;
2. Department of Materials Science and Engineering, Anadolu University, Eskisehir, Turkey;
3. Material Science and Engineering Programme, Sabanci University, Istanbul, Turkey

摘　要：采用无压熔渗法将 Al/Al 合金渗透到多孔 α-Si_3N_4 中，并对 AlN−Si−Al 复合材料在 50~300 °C 的热性能进行研究。SEM 和 TEM 结果表明，AlN 的晶粒尺寸小于 1 μm，另外，AlN−Si−Al 复合材料还表现出较高的热导率 55~107 W/(m·K)。采用热导率为 107 W/(m·K)的商用 Al 得到的 AlN−Si−Al 复合材料的热膨胀系数为 $6.5\times10^{-6}K^{-1}$。Al 的热膨胀系数高达 $23.6\times10^{-6}K^{-1}$，而 AlN−Si−Al 复合材料却具有低的热膨胀系数，其原因是在渗透过程中形成了 Si 和 AlN。

关键词：AlN；陶瓷基复合材料；热性能；金属溶渗

(Edited by Hua YANG)